

# Random lasing from granular surface of waveguide with blends of PS and PMMA

Xuanke Zhao,<sup>1,2</sup> Zhaoxin Wu,<sup>1,\*</sup> Shuya Ning,<sup>1</sup> Shixiong Liang,<sup>1</sup> Dawei Wang,<sup>1</sup>  
Xun Hou<sup>1</sup>

<sup>1</sup> Key Laboratory of Photonics Technology for information, Key Laboratory for Physical Electronics and Devices of the Ministry of Education, School of Electronic and Information Engineering, Xi'an Jiaotong University, Xi'an 710049, China;

<sup>2</sup> Dept. of Physics, Xi'an Research Inst. of Hi-Tech, Hongqing Town, Xi'an 710025, China  
\*zhaoxinwu@mail.xjtu.edu.cn

**Abstract:** Lasing from a planar waveguide with the blend of Polystyrene(PS): Poly-methylmethacrylate(PMMA) doped with tris(8-hydroxyquinolino)aluminum(Alq<sub>3</sub>) and 4-(dicyanomethylene)-2-tert-butyl-6(1,1,7,7-tetramethyljulolidyl-9-enyl)-4H-pyran(DCJTB) was investigated. Due to phase separation of the blend of PS:PMMA during the solvent evaporation process, a waveguide with granular surface was obtained, which has 2D island-like nanostructures with diameters ranging between 200 and 400 nm and heights at about 25 nm. Pumped by a YAG laser with wavelength of 355nm, a significant random lasing was observed. Compared to the amplified spontaneous radiation (ASE) of planar waveguides with only PMMA or PS doped with Alq<sub>3</sub>:DCJTB prepared under the same conditions, the lasing threshold of the former is decreased by about 5 times, and the full width at half maximum (FWHM) is reduced to 1.7nm from 12~15 nm. Our experiments show a promising method to achieve lower threshold for organic lasers.

©2011 Optical Society of America

**OCIS codes:** (140.0140) Laser and laser optics; (140.5960) Semiconductor lasers; (230.7390) Waveguides:planar; (290.4210) Multiple scattering.

---

## References and links

1. N. M. Lawandy, R. M. Balachandran, A. S. L. Gomes, and E. Sauvain, "Laser action in strongly scattering media," *Nature* **368**(6470), 436–438 (1994).
2. H. Cao, Y. G. Zhao, S. T. Ho, E. W. Seelig, Q. H. Wang, and R. P. H. Chang, "Random laser action in semiconductor powder," *Phys. Rev. Lett.* **82**(11), 2278–2281 (1999).
3. D. S. Wiersma, "The smallest random laser," *Nature* **406**(6792), 132–135 (2000).
4. V. M. Apalkov, M. E. Raith, and B. Shapiro, "Random resonators and prelocalized modes in disordered dielectric films," *Phys. Rev. Lett.* **89**(1), 016802 (2002).
5. D. S. Wiersma, "The physics and applications of random lasers," *Nat. Phys.* **4**(5), 359–367 (2008).
6. Q. Song, S. Xiao, Z. Xu, V. M. Shalaev, and Y. L. Kim, "Random laser spectroscopy for nanoscale perturbation sensing," *Opt. Lett.* **35**(15), 2624–2626 (2010).
7. V. M. Markushev, N. E. Ter-Gabrielyan, M. Briskina Ch, V. R. Belan, and V. F. Z. Sov, "Stimulated emission kinetics of neodymium powder lasers," *J. Quantum Electron* **20**(7), 773–777 (1990).
8. D. Anglos, A. Stassinopoulos, R. N. Das, G. Zacharakis, M. Psyllaki, R. Jakubiak, R. A. Vaia, E. P. Giannelis, and S. H. Anastasiadis, "Random laser action in organic–inorganic nanocomposites," *J. Opt. Soc. Am. B* **21**(1), 208–213 (2004).
9. T. Takahashi, T. Nakamura, and S. Adachi, "Blue-light-emitting ZnSe random laser," *Opt. Lett.* **34**(24), 3923–3925 (2009).
10. G. Zacharakis, N. A. Papadogiannis, and T. G. Papazoglou, "Random lasing following two-photon excitation of highly scattering gain media," *Appl. Phys. Lett.* **81**(14), 2511–2513 (2002).
11. E. Pecoraro, S. García-Revilla, R. A. S. Ferreira, R. Balda, L. D. Carlos, and J. Fernández, "Real time random laser properties of Rhodamine-doped di-ureasil hybrids," *Opt. Express* **18**(7), 7470–7478 (2010).
12. S. V. Frolov, Z. V. Vardeny, K. Yoshino, A. A. Zakhidov, and R. H. Baughman, "Stimulated emission in high gain organic media," *Phys. Rev. B* **59**(8), R5284–R5287 (1999).
13. R. C. Polson, A. Chipoline, and Z. V. Vardeny, "Random lasing in  $\pi$ -conjugated films and infiltrated opals," *Adv. Mater. (Deerfield Beach Fla.)* **13**(10), 760–764 (2001).
14. R. M. Balachandran, D. P. Pacheco, and N. M. Lawandy, "Laser action in polymeric gain media containing scattering particles," *Appl. Opt.* **35**(4), 640–643 (1996).

15. A. Tulek, R. C. Polson, and Z. V. Vardeny, "Naturally occurring resonators in random lasing of  $\pi$ -conjugated polymer films," *Nat. Phys.* **6**(4), 303–310 (2010).
16. H. Cao, Y. Ling, J. Y. Xu, C. Q. Cao, and P. Kumar, "Photon statistics of random lasers with resonant feedback," *Phys. Rev. Lett.* **86**(20), 4524–4527 (2001).
17. M. N. Shkunov, M. C. DeLong, M. E. Raikh, Z. V. Vardeny, A. A. Zakhidov, and R. H. Baughman, "Photonic versus random lasing in opal single crystals," *Synth. Met.* **116**(1-3), 485–491 (2001).
18. D. S. Wiersma and S. Cavalieri, "Light emission: A temperature-tunable random laser," *Nature* **414**(6865), 708–709 (2001).
19. C. Bouvy, E. Chelnokov, R. Zhao, W. Marine, R. Sporcken, and B.-L. Su, "Random laser action of ZnO@mesoporous silicas," *Nano.Technol.* **19**, 105710 (2008).
20. C.-R. Lee, S.-H. Lin, C.-H. Guo, S.-H. Chang, T.-S. Mo, and S.-C. Chu, "All-optically controllable random laser based on a dye-doped polymer-dispersed liquid crystal with nano-sized droplets," *Opt. Express* **18**(3), 2406–2412 (2010).
21. R. C. Polson and Z. V. Vardeny, "Organic random lasers in the weak-scattering regime," *Phys. Rev. B* **71**(4), 045205 (2005).
22. Q. Song, L. Liu, L. Xu, Y. Wu, and Z. Wang, "Electrical tunable random laser emission from a liquid-crystal infiltrated disordered planar microcavity," *Opt. Lett.* **34**(3), 298–300 (2009).
23. Y. Chen, J. Herrnsdorf, B. Guilhabert, Y. Zhang, I. M. Watson, E. Gu, N. Laurand, and M. D. Dawson, "Colloidal quantum dot random laser," *Opt. Express* **19**(4), 2996–3003 (2011).
24. K. Tanaka, A. Takahara, and T. Kajiyama, "Film Thickness Dependence of the Surface Structure of Immiscible Polystyrene/Poly(methyl methacrylate) Blends," *Macromolecules* **29**(9), 3232–3239 (1996).
25. W. L. Barnes and P. Andrew, "Energy transfer under control," *Nature* **400**(6744), 505–506 (1999).
26. M. Koschorreck, R. Gehlhaar, V. G. Lyssenko, M. Swoboda, M. Hoffmann, and K. Leo, "Dynamics of a high-Q vertical-cavity organic laser," *Appl. Phys. Lett.* **87**(18), 181108 (2005).
27. C. Ton-That, A. G. Shard, R. Daley, and R. H. Bradley, "Effects of Annealing on the Surface Composition and Morphology of PS/PMMA Blend," *Macromolecules* **33**(22), 8453–8459 (2000).
28. L. Fang, M. Wei, C. Barry, and J. Mead, "Effect of Spin Speed and Solution Concentration on the Directed Assembly of Polymer Blends," *Macromolecules* **43**(23), 9747–9753 (2010).

## 1. Introduction

Random lasers, which are formed by strong scattering in disordered gain systems, have attracted much attention in both theoretical and experimental areas for their potential applications as micrometer-scale laser sources, as remote sensors, and in optical storage [1–6], because of their extreme simplicity, low cost and robustness in operation. Many optical materials were reported for the random lasing, such as powders of solid-state luminescent and laser crystals [7–9], liquid laser dyes with scatterers [10,11], polymeric films with and without intentionally introduced scatterers [12–15], ZnO scattering films and nanoclusters [2,16], dye-infiltrated opals [13,17], porous media infiltrated with liquid crystals with dyes [18–20] and many others [21–23].

In this Letter, we reported random lasing emission from a waveguide with a granular surface made of spin-coated Polystyrene(PS): Poly-methylmethacrylate(PMMA): tris(8-hydroxyquinolino)aluminum( $\text{Alq}_3$ ):4-(dicyanomethylene)-2-tert-butyl-6(1,1,7,7-tetramethyljulolidyl-9-enyl)-4H-pyran(DCJTb) blend film. PS/PMMA blend is a well-known immiscible combination, whose bulk and surface phase separation has been observed since 1996 [24]. By spin-coating process, without doping nanoparticles in host materials, we obtained a 2D granular nanostructure with diameters of about 200–400 nm and heights of about 25 nm due to phase separation of PS/PMMA during the solvent evaporation process. Compared to the waveguides with only PS or PMMA doped by dyes, the waveguide of the blend of PS:PMMA doped by dyes exhibited excellent random lasing action with lower threshold.

## 2. Sample preparation and experimental setups

The samples were fabricated as follows: First, chloroform was used to prepare the polymer solutions of PS, PMMA and their blends doped by  $\text{Alq}_3$  and DCJTb with solution concentration of 20mg/ml. The ratios of polymer solutions are 100:100:3.5wt for the PS or PMMA doped with  $\text{Alq}_3$ :DCJTb, and the ratio of for the blends of PMMA and PS as host was optimized to be 30:70:100:3.5wt. Then, the planar waveguide were prepared by spin-casting blend solutions under ambient conditions onto a glass substrate, which was rotated at 2000 r.p.m for 30 second, and finally, the spin-coated films were annealed at 70°C (slightly greater than the boiling point

of chloroform and lower than glass transition temperatures of PS and PMMA) for 30 minutes in an oven. The structures of three samples prepared are shown as the follows:

Sample A: glass/PS:Alq<sub>3</sub>:DCJTB(100:100:3.5wt)/air

Sample B: glass/PMMA:Alq<sub>3</sub>:DCJTB(100:100:3.5wt)/air

Sample C: glass/PS:PMMA:Alq<sub>3</sub>:DCJTB(30:70:100:3.5wt)/air

Among them, Sample A and B were used as control devices to compare with Sample C. In these samples, the glass substrate, polymer layer and air formed an asymmetric three-layer planar waveguide. Film thickness and refractive index of the three samples were measured by Ellipsometry (SE MF-1000, Korea). Surface topography of the films was characterized by an AFM (NT-MDT, Russia) under ambient conditions. PS ( $M_w=250K$ ) and PMMA ( $M_w=350K$ ) obtained from ACROS and Alfa Aesar, whose glass transition temperatures were 93°C and 150 °C respectively, were used in the experiment.

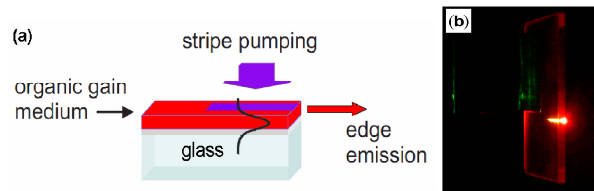


Fig. 1. (a) Schematic illustration of configuration of PS:PMMA:Alq<sub>3</sub>:DCJTB waveguide and excitation-detection. (b) A photograph of emission when the pump energy is above threshold.

The samples were pumped by a YAG laser (355nm/5.55ns/10Hz) (Surelite I, Continuum Corp., USA). Through a pinhole filter, a slit and a cylindrical lens, the laser beam formed a stripe with the size of 7mm×1mm, and was perpendicular to the surface of the samples. Edge emission spectra were measured by Fiber Optic Spectrometer (Ocean Optics SpectraSuite, USB2000), as shown in Fig. 1(a). Figure 1(b) shows a photograph of the emission when the pump energy is above threshold. The lasing FWHM, threshold and peak quality factor (Q value) were measured. All measurements were carried out under ambient environment.

### 3. Results and discussion

In our experiments, we chose Alq<sub>3</sub> doped laser dye DCJTB as the gain medium. The PL spectrum of Alq<sub>3</sub> and absorption spectrum of DCJTB possess larger overlap, indicating that the effective Forster energy transfer from Alq<sub>3</sub> to DCJTB should exist. By doping DCJTB into Alq<sub>3</sub>, the concentration quenching effect is reduced, and the distance between emission peak and absorption peak is wider, so the self-absorption is avoided and the laser threshold is also greatly reduced [25,26].

The refractive index of the glass substrate is 1.51. The thickness and refractive index of the three samples measured by Ellipsometry were shown in Table 1, which are greater than the refractive index of glass( $n=1.51$ ) and air ( $n=1.0$ ). Thus, the glass substrate, organic thin film layer and air formed an asymmetric three-layer planar waveguide.

**Table 1. The Thickness and Refractive Index of the Three Samples.**

Samples	Thickness(nm)	Refractive index
Sample A: glass/PS:Alq <sub>3</sub> :DCJTB	264.2	1.59
Sample B: glass/PMMA:Alq <sub>3</sub> :DCJTB	274.6	1.60
Sample C: glass/PS:PMMA:Alq <sub>3</sub> :DCJTB	210.7~231.1*	1.58~1.61*

\*The measured value of the different areas.

Figure 2 shows the surface morphologies of the three samples measured by AFM. The surface of Samples A and B is quite smooth (whose RMS roughness is 0.29nm and 0.24nm,

respectively), while that of Sample C is granular, which has 2D island-like nanostructures with diameters ranging between 200 and 400 nm and heights at about 25 nm. Figure 2 (c2) is the 3D AFM image of sample C. The island- and sea-like matrixes in Fig. 2(c1) and (c2) were composed of PMMA- and PS-rich phases, in which the island-like is PMMA-rich phase and the sea-like is PS-rich phase, respectively. During the spin-casting process, since the solvent evaporates relatively fast, the polymer chains are generally frozen in the thin films before reaching a thermodynamically stable state. Although PS has a marginally lower surface free energy than PMMA, due to a higher solubility of the PMMA in the chloroform, PS is more quickly depleted from the solvent and solidifies first onto the substrate and PMMA tends to stay longer in the liquid phase and forms a second layer at the surface [24,27,28], thus forming a granular surface structure on the glass substrate.

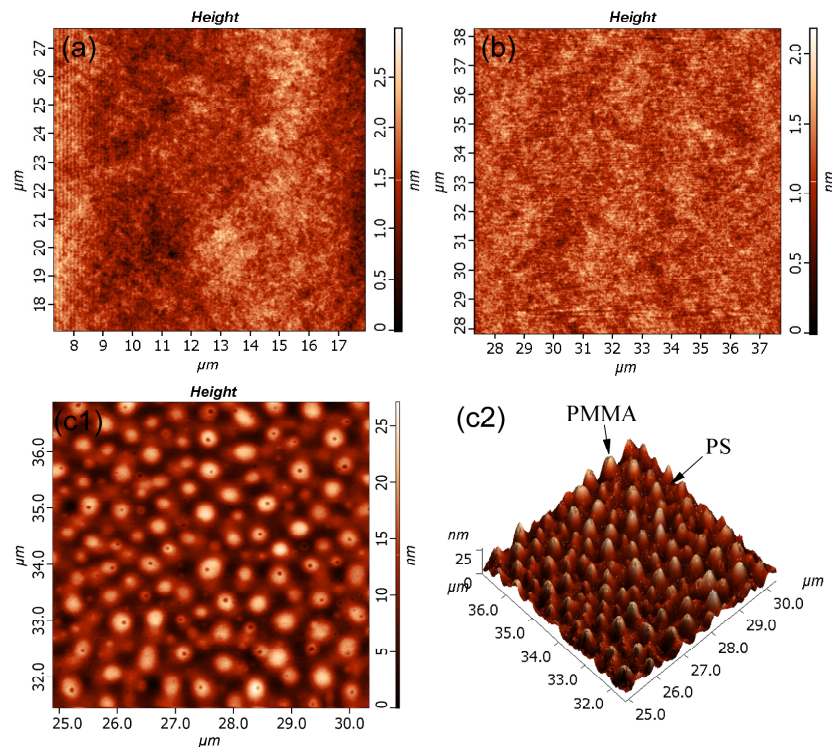


Fig. 2. AFM images of the three samples: (a) Sample A, (b) Sample B and, (c1,c2) Sample C

Figure 3 shows how the pump energy can affect ASE spectra, input-output intensity and FWHM of Samples A, B and C. Clearly, as shown in Fig. 3(a2), there is a threshold about  $1.86\text{mJ}/\text{cm}^2$  in the input-output curve of Sample A. Above this threshold, the FWHM drops from  $\sim 150\text{nm}$  of PL Spectroscopy to about  $15\text{nm}$ . Similar to Sample A, as shown in Fig. 3(b2), there is a clear threshold in the input-output curve of Sample B too, and the threshold is about  $1.80\text{mJ}/\text{cm}^2$ ; above the pump energy threshold, the FWHM drops to about  $12\text{nm}$ , slightly narrower than that of Sample A. This is probably because Sample B is slightly thicker than Sample A and the refractive index of Sample B is slightly greater than that of Sample A, so there is a slightly larger gain and waveguide constraint of light radiation, resulting in an decrease of ASE threshold and FWHM.

The lasing action of Sample C was shown in Fig. 3(c1). The main differences of Sample C and Samples A and B is that there are many sharp peaks in the emission spectra from Sample C, instead of the smooth line profiles shown in Fig. 3(a1) and Fig. 3(b1). The wavelength of the

sharp peaks depends on the sample position we choose to excite, which is a distinct signature of random lasing actions. Figure 3(c2) clearly shows a threshold behavior: above the pump threshold, multiple sharp peaks emerged in the emission spectrum, and the emission intensity increased much more rapidly with the pump power. The lasing threshold is about  $341.6\mu\text{J}/\text{cm}^2$ , far less than that of Samples A and B, and the laser FWHM above threshold is reduced to  $1.7\text{nm}$ , far narrower than that of Samples A and B too. Limited by the spectral resolution ( $0.35\text{nm}$ ) of Fiber Optic Spectrometer used in our experiment, the smaller details of the spectrum cannot be observed. Figure 4 shows the edge emission spectra at different excitation intensity, from which significant characteristics of random lasing can be observed clearly.

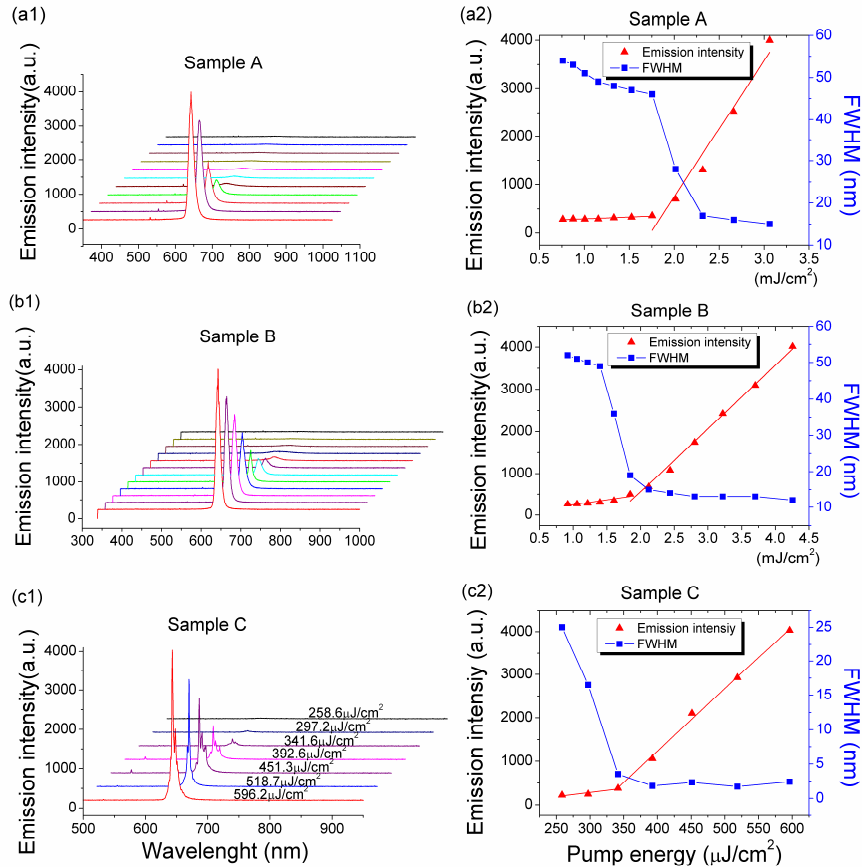


Fig. 3. Edge emission spectra, intensity and FWHM of the three samples plotted as a function of pump energy

The highest peak of each emission spectra in Fig. 4 was measured, the peak wavelength, FWHM, and the quality factor ( $Q$  value) of random laser peak was calculated too, the calculated results are shown in Table 2. As can be seen from Table 2, below the laser threshold, the FWHM of spectra is wide and the  $Q$  value of each peak is low; above the laser threshold, the FWHM decreases rapidly, and the  $Q$  value factor increases rapidly to the maximum value  $380.79$  (limited by spectrometer resolution), almost 7-9 times larger than the highest quality factors ( $43.33$  and  $53.68$ , respectively) of Samples A and B, while the laser threshold is reduced to about  $1/5$  of Samples A and B. In addition, we also found that the laser wavelength has a little blue-shift with the increase of excitation intensity in Sample C. It maybe due to getting enough gain with shorter scattering path at higher excitation intensity, and form a corresponding shorter random micro-cavity which leads to a blue-shift of laser wavelength.

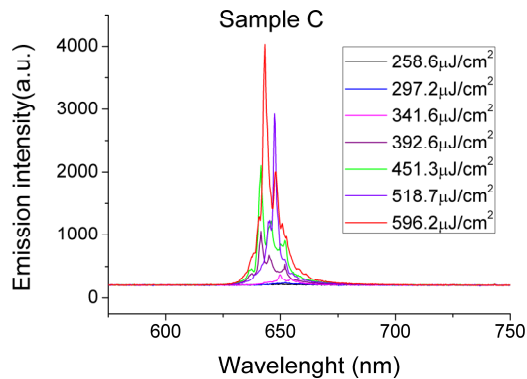


Fig. 4. Random lasing action of Sample C with the increase of excitation intensity

**Table 2. The Peak Wavelength, FWHM and Quality Factor of Random Laser of Sample C.**

$\lambda_p$ (nm)	650.45	652.16	649.76	641.15	641.50	647.35	643.22
FWHM( $\Delta\lambda$ )(nm)	25.0	16.5	3.5	1.8	2.2	1.7	2.3
$Q(\lambda_p/\Delta\lambda)$	26.02	39.52	185.65	356.19	291.59	380.79	279.66

The random lasing in Sample C was considered to be from the random scattering generated by 2D granular nanostructure on the surface of the waveguide, which arise from phase separation of PS/PMMA blend. Because of the short scattering mean free path in the PS/PMMA blend film, the emitted light is strongly scattered, and closed loop paths can be formed through multiple scattering. These loops could serve as ring cavities for light and the ring cavities formed by recurrent scattering have different loss. When the pump intensity increases, the gain reaches the loss first in the low-loss cavities. Then laser oscillation occurs in other cavities, and the lasing wavelengths are determined by the cavity resonances. Laser emission from these resonators results in a small number of discrete narrow peaks in the emission spectrum. This is similar to ZnO powder thin film prepared by Cao et al. [2,16]. Apart from the trapping of light by multiple scattering, the additional feedback from the surface boundaries of the samples is expected to be an important factor [3]. Compared to the previous reports, such as the random lasing from the nano-particles, ZnO, TiO<sub>2</sub>, SiO<sub>2</sub>, and so on, the scattering centers in the blends of PS:PMMA were easily formed especially on the larger area planar waveguide for the further random lasers with lower cost. In addition, the laser characteristics can be easily tuned by varying the shape and size of the granules on the waveguide surface.

#### 4. Conclusion

In summary, we reported random lasing emission from a waveguide with a granular surface made of spin-coated PS:PMMA:Alq<sub>3</sub>:DCJTb blend film due to phase separation of PS/PMMA during the solvent evaporation process. Compared to the ASE of planar waveguides of PMMA or PS doped by Alq<sub>3</sub>:DCJTb prepared under the same conditions, the lasing threshold of the former decreased by about 5 times, and the FWHM is reduced to 1.7 nm from 12~15 nm. Our demonstration showed a simple and easy way to achieve organic random lasing with the lower threshold for the further applications.